

# Microbial paracetamol degradation involves a high diversity of novel amidase enzyme candidates

Ana B. Rios-Miguel<sup>a,\*</sup>, Garrett J. Smith<sup>a</sup>, Geert Cremers<sup>a</sup>, Theo van Alen<sup>a</sup>, Mike S.M. Jetten<sup>a,b</sup>, Huub J.M. Op den Camp<sup>a</sup>, Cornelia U. Welte<sup>a,b,\*</sup>

<sup>a</sup> Department of Microbiology, Radboud University, Radboud Institute for Biological and Environmental Sciences, Heyendaalseweg 135, Nijmegen 6525 AJ, the Netherlands

<sup>b</sup> Soehngen Institute of Anaerobic Microbiology, Radboud University, Heyendaalseweg 135, Nijmegen 6525 AJ, the Netherlands

## ARTICLE INFO

### Keywords:

Amidase evolution  
Deaminase  
Dioxygenase  
Metagenomics  
Mobile genetic elements  
*Pseudomonas*

## ABSTRACT

Pharmaceuticals are relatively new to nature and often not completely removed in wastewater treatment plants (WWTPs). Consequently, these micropollutants end up in water bodies all around the world posing a great environmental risk. One exception to this recalcitrant conversion is paracetamol, whose full degradation has been linked to several microorganisms. However, the genes and corresponding proteins involved in microbial paracetamol degradation are still elusive. In order to improve our knowledge of the microbial paracetamol degradation pathway, we inoculated a bioreactor with sludge of a hospital WWTP (Pharmafilter, Delft, NL) and fed it with paracetamol as the sole carbon source. Paracetamol was fully degraded without any lag phase and the enriched microbial community was investigated by metagenomic and metatranscriptomic analyses, which demonstrated that the microbial community was very diverse. Dilution and plating on paracetamol-amended agar plates yielded two *Pseudomonas* sp. isolates: a fast-growing *Pseudomonas* sp. that degraded 200 mg/L of paracetamol in approximately 10 h while excreting 4-aminophenol, and a slow-growing *Pseudomonas* sp. that degraded paracetamol without obvious intermediates in more than 90 days. Each *Pseudomonas* sp. contained a different highly-expressed amidase (31% identity to each other). These amidase genes were not detected in the bioreactor metagenome suggesting that other as-yet uncharacterized amidases may be responsible for the first biodegradation step of paracetamol. Uncharacterized deaminase genes and genes encoding dioxygenase enzymes involved in the catabolism of aromatic compounds and amino acids were the most likely candidates responsible for the degradation of paracetamol intermediates based on their high expression levels in the bioreactor metagenome and the *Pseudomonas* spp. genomes. Furthermore, cross-feeding between different community members might have occurred to efficiently degrade paracetamol and its intermediates in the bioreactor. This study increases our knowledge about the ongoing microbial evolution towards biodegradation of pharmaceuticals and points to a large diversity of (amidase) enzymes that are likely involved in paracetamol metabolism in WWTPs.

## 1. Introduction

Hundreds of pharmaceutical compounds are being detected at low concentrations in water bodies all around the world posing a severe risk to the environment and to human health (Gavrilescu et al., 2015; Wilkinson John et al., 2022). The consumption of medication and personal

care products will most likely increase in the future. Therefore, there is an urgent need to develop new technologies able to remove these chemicals at low concentrations before reaching the environment. Until now, cost-efficient removal of common pollutants (i.e. ammonium-nitrogen) has been achieved using microorganisms in wastewater treatment plants (WWTPs). As large-scale use of

**Abbreviations:** WWTP, wastewater treatment plant; MBR, membrane bioreactor; GAC, granular activated carbon; APAP, N-acetyl-p-aminophenol or paracetamol; 4-AP, 4-aminophenol; HQ, hydroquinone; HRT, hydraulic retention time; SRT, solid retention time; Pfast, *Pseudomonas* sp. isolate growing fast on APAP as sole carbon source; Pslow, *Pseudomonas* sp. isolate growing slow on APAP as sole carbon source; HGT, horizontal gene transfer; MAG, metagenome-assembled genome; TPM, transcripts per million.

\* Corresponding authors at: Department of Microbiology, Radboud University, Radboud Institute for Biological and Environmental Sciences, Heyendaalseweg 135, Nijmegen 6525 AJ, the Netherlands.

E-mail addresses: [a.riosmiguel@science.ru.nl](mailto:a.riosmiguel@science.ru.nl) (A.B. Rios-Miguel), [c.welte@science.ru.nl](mailto:c.welte@science.ru.nl) (C.U. Welte).

<https://doi.org/10.1016/j.wroa.2022.100152>

Received 13 May 2022; Received in revised form 13 July 2022; Accepted 3 August 2022

Available online 4 August 2022

2589-9147/© 2022 The Authors. Published by Elsevier Ltd. This is an open access article under the CC BY license (<http://creativecommons.org/licenses/by/4.0/>).

pharmaceuticals has only recently resulted in discharge to many different environments, the metabolic pathways of their conversion (at relatively low concentrations) might not have evolved yet or might not be very efficient.

Acetaminophen (N-acetyl-p-aminophenol, APAP), more commonly known as paracetamol, is one of the most consumed analgesic drugs worldwide (Wu et al., 2012). Consequently, its concentration in wastewater and surface waters is among the highest of all pharmaceutical micropollutants. APAP concentration can reach more than 100 µg/L in WWTP influents and more than 100 ng/L in rivers (Kanama et al., 2018; Wilkinson et al., 2022; Wu et al., 2012; Watson database - <https://data.emissieregistratie.nl/watson>). Unlike many other pharmaceuticals, APAP is degraded by microorganisms and is often well removed in WWTPs. Several microorganisms have been related to APAP degradation in activated sludge and soil samples (i.e. *Penicillium*, *Pseudomonas*, *Flavobacterium*, *Dokdonella*, *Ensifer*, *Delftia*) (Hart and Orr, 1974; Palma et al., 2018; Park and Oh, 2020a; b; Rios-Miguel et al., 2021; Žur et al., 2018a). However, the genomes of these microorganisms have not yet been reported and therefore, the responsible genes and mechanisms for APAP biodegradation in WWTPs are not yet known.

4-Aminophenol (4-AP) and hydroquinone (HQ) have been measured in several APAP biodegradation experiments (Park and Oh, 2020a; b; Zhang et al., 2013). Consequently, an aryl acylamidase, a deaminase, and hydroquinone 1,2-dioxygenase were proposed as enzymes potentially involved in the biodegradation pathway of APAP (Grignat et al., 2022; Lee et al., 2015; Žur et al., 2018b). In fact, five amidases have been shown to transform APAP to 4-AP or to a brown compound (Supplementary Table S1) (Chen et al., 2016; Ko et al., 2010; Lee et al., 2015; Yun et al., 2017; Zhang et al., 2012, 2020, 2019). Besides, 1,2,4-trihydroxybenzene could be an intermediate of APAP degradation since it was measured in a *Burkholderia* sp. degrading 4-AP (Takenaka et al., 2003). Despite this knowledge, the exact genes/enzymes that microorganisms are using for APAP biodegradation in the environment are currently unknown.

To fill this gap, we analyzed the APAP-degrading microbial community from a hospital WWTP by metagenomics and metatranscriptomics. Furthermore, we were able to isolate two *Pseudomonas* species from the bioreactor that were capable of growing on APAP. Our aim was to identify the genes involved in APAP biodegradation and determine the genomic location and organization of these genes (clusters) in different microorganisms. These results will help to understand the evolution of microbial metabolism towards biodegradation of pharmaceuticals and will provide molecular biomarkers to screen environments for APAP-degrading microorganisms.

## 2. Methods

### 2.1. Sampling and bioreactor set-up

Biomass was obtained from a membrane bioreactor (MBR) and a granular activated carbon (GAC) process at the Pharmafilter WWTP in Delft, the Netherlands, on 1-2-2021. This plant treats wastewater and solid waste from the Reinier de Graaf hospital, in Delft, and consists of an anaerobic-anoxic-oxic MBR, an ozonation tank, and a GAC treatment (<https://www.stowa.nl/publicaties/evaluation-report-pharmafilter>). A laboratory-scale membrane bioreactor (1.5 L) was inoculated with 15 mL of the MBR biomass and 15 mL of the GAC biomass. The same inoculum was autoclaved for 20 min at 121 °C and incubated with 50 mg/L of APAP to investigate its adsorption to biomass. The sludge without heat inactivation was also tested in the experiment. The lab-scale membrane and bioreactor vessel were built at Radboud University technical center. The bioreactor appliances were from Applikon Biotechnology B.V. (Delft, The Netherlands). The membrane consisted of an integral immersed Zenon ZW-1 module with 0.04 µm pore-sized hollow fibers from Suez Water Technologies & Solutions (Feasterville-Trevoise, USA). It was never backwashed or replaced during the

experiment. The bioreactor was fed with synthetic medium containing 0.05-0.4 g/L APAP (Merck, ≥99.0%, Darmstadt, Germany) as sole carbon source, 0.2 g/L K<sub>2</sub>HPO<sub>4</sub>, 0.1 g/L KH<sub>2</sub>PO<sub>4</sub>, 0.06 g/L NH<sub>4</sub>Cl, 0.01 g/L MgSO<sub>4</sub> × 7 H<sub>2</sub>O, 0.01 g/L CaCl<sub>2</sub>, and trace elements solution (Rios-Miguel et al., 2021). Since APAP was degraded very fast, the organic loading rate was increased over the first 38 days from 0.022 to 0.227 mg APAP/min. This was done by increasing the concentration of APAP in the medium to 400 mg/L and by reducing the hydraulic retention time (HRT) from 2.4 to 1.8 d (Fig. 1). When bacterial growth became exponential, the solid retention time (SRT) was set to 10 d to reach a steady state. After about 90 d, the HRT was set to 3.7 d to determine the microbial community changes at lower APAP loading rates (Fig. 1). Furthermore, the bioreactor was run in the dark at constant 500 rpm stirring, a pH value of 7, an airflow rate of 30 ml/min, and room temperature (20 ± 1 °C). A pH sensor was connected to a controller that activated a KHCO<sub>3</sub> base pump to keep the pH stable at 7.

### 2.2. Bioreactor monitoring: total suspended solids, paracetamol, 4-aminophenol, and hydroquinone concentration, DNA and RNA sequencing

Total suspended solids (TSS) were regularly measured by passing 30 mL of the sample through a 0.45 µm pore size glass-fiber filter which was dried overnight at 105 °C. Samples (2 mL) were taken regularly from the bioreactor in triplicates, centrifuged, and stored at -20 °C (both supernatant and pellet) until APAP, 4-AP, HQ, and DNA analysis. APAP, 4-AP, and HQ were measured in the supernatant using an HPLC-UV (Agilent Technologies 1000 series, injection volume of 100 µL; a mobile phase of acetate 1%: methanol (9:1); flow rate 1200 µl/min; and a C18 reverse-phase column: LiChrospher® 100 RP-18 (5 µm) LiChroCART® 125-4, 12.5 cm × 4 mm, Merck, Darmstadt, Germany). The retention times of APAP, 4-AP, and HQ were 4.4, 1.7, and 2.3 min, respectively. Furthermore, APAP concentration was measured at a wavelength of 249 nm, and 4-AP and HQ at 280 nm. DNA was extracted from the pellets using the DNeasy PowerSoil Kit (Qiagen Benelux B.V.) following manufacturer's instructions. The samples were submitted to Macrogen (Seoul, South Korea) for amplicon sequencing of the V3 and V4 regions of the bacterial 16S rRNA gene (primers Bac341F and Bac785R (Klindworth et al., 2013)) using an Illumina MiSeq. Six samples of 30 mL were taken at day 77 (two weeks after SRT was set to 10 d and the bioreactor was in a steady state). Three samples were centrifuged and stored at -20 °C for DNA sequencing and the other three were frozen in liquid nitrogen and stored at -80 °C for RNA sequencing. DNA was extracted using the DNeasy PowerSoil Kit (Qiagen Benelux B.V.) and sequenced at BaseClear (Leiden, The Netherlands). RNA was extracted using the RNeasy PowerSoil Total RNA Kit (Qiagen Benelux B.V.) with an extra DNase treatment from Ribopure™ Kit (Thermo Fisher Scientific, Waltham, MA USA). Ribosomal RNA was removed using the Microbexpress kit (Life Technologies, Carlsbad, USA) and rRNA depleted samples were submitted to Macrogen (Seoul, South Korea) for sequencing. DNA and RNA samples were sequenced using Illumina Novaseq technology. All DNA and RNA quantities were determined using the Qubit dsDNA/RNA HS Assay Kit (Thermo Fisher Scientific, Waltham, MA USA) and a Qubit fluorometer (Thermo Fisher Scientific, Waltham, MA USA). Furthermore, DNA and RNA quality was checked with the Agilent 2100 Bioanalyzer and the High sensitivity DNA/RNA kit (Agilent, Santa Clara, USA).

### 2.3. Isolation and DNA/RNA sequencing of bacteria growing on paracetamol

We performed serial dilutions of the bioreactor biomass in synthetic medium (same as the bioreactor) with APAP as sole carbon source (0.2-0.4 g/L). The biomass of the most highly diluted culture displaying APAP biodegradation was plated on agar-solidified medium with APAP as sole carbon source. This solid medium consisted of the bioreactor synthetic medium, 0.4 g/L of APAP, and 1.5% w/v bacteriological agar

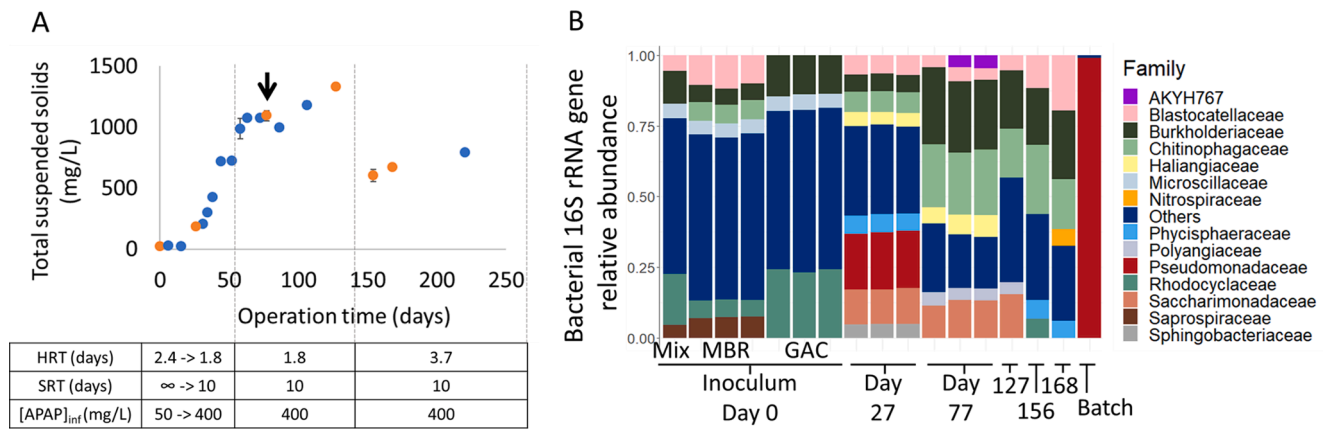


**Fig. 1.** A: Total suspended solids in mg/L. Orange dots represent the time points when 16S rRNA genes were sequenced. The black arrow represents the time point when whole-genome and transcriptome sequencing occurred. B: relative abundance of bacterial 16S rRNA genes in the inoculum and the bioreactor at several time points. Batch sample represents the serial dilution of the bioreactor biomass in medium containing 400 mg/L of APAP. Abbreviations: HRT, hydraulic retention time; SRT, solid retention time; APAP, paracetamol; MBR, membrane bioreactor; GAC, granular activated carbon; Mix, mixture of MBR and GAC.

(VWR, Belgium). Brown and white colonies, designated as Pfast and Pslow, respectively, were found in the agar plates. Both colonies were used to inoculate bottles containing synthetic bioreactor medium with 200 mg/L APAP as sole carbon source. One milliliter of these cultures was used as inoculum for triplicate-bottle experiments where APAP biodegradation kinetics were measured and the DNA and RNA of the bacteria were sequenced. DNA and RNA from both isolates were extracted as described above, except for the Pfast DNA extraction for ONT sequencing, which was performed at Baseclear with the Wizard HMW DNA Extraction kit (Promega Benelux B.V., Leiden, The Netherlands). The genome of the fast-growing isolate Pfast was sequenced using Illumina Novaseq and ONT GridION at Baseclear (Leiden, The Netherlands). RNA of this isolate was sequenced using Illumina Novaseq, also at Baseclear. Only one of the 3 RNA samples could be sequenced. The genome and transcriptome of the slow-growing isolate Pslow were sequenced using an in-house Illumina MiSeq. For DNA library preparation the Nextera XT kit was used and for transcriptomic library preparation, the TruSeq Stranded mRNA kit was used according to the manufacturer's instructions (Illumina, San Diego, USA). All DNA and RNA quantifications and quality checks were performed as described above (Qubit and Bioanalyzer). For genomic DNA libraries, 300 bp paired-end sequencing was performed and for the transcriptomes, 150 bp single-read sequencing was done, using the Illumina MiSeq sequencing machine (Illumina, San Diego, California). The raw sequence data and metadata of the bioreactor and isolates have been deposited at the read sequence archive (SRA) database of the NCBI under the BioProject ID PRJNA831879.

## 2.4. Bioinformatic analysis

### 2.4.1. 16S rRNA gene sequencing data analysis

Analysis of the 16S rRNA sequencing output files was performed within R version 3.4.1 (Team, 2013) using the DADA2 pipeline (Callahan et al., 2016). Taxonomic assignment of the reads was up to the species level when possible using the Silva non-redundant database version 128 (Yilmaz et al., 2014). Count data were normalized to relative abundances. Data visualization and analysis were performed using phyloseq and ggplot packages (McMurdie and Holmes, 2013; Wickham and Wickham, 2007). Chao1, Simpson and Shannon diversity indices were calculated using the estimate richness function of the phyloseq package.

### 2.4.2. DNA assembly, binning, and annotation

The quality of the metagenome sequencing data was assessed using FASTQC before and after quality processing. Quality-trimming, adapter

removal and contaminant filtering of Illumina paired-end sequencing reads was performed using BBDuk (BBTools, DOE Joint Genome Institute, Lawrence Berkeley National Laboratory, USA). The DNA trimmed reads were assembled using MetaSpades and aligned to the assembly using BBMap to generate coverage information (Nurk et al., 2017). The assemblies were binned using different binning algorithms (BinSanity, CONCOCT, MaxBin 2.0, and MetaBAT 2) (Alneberg et al., 2014; Graham et al., 2017; Kang et al., 2019; Wu et al., 2015). DAS Tool was used for consensus binning (Sieber et al., 2018). GTDB-Tk was used to assign taxonomy and CheckM was used to assess the quality of the bins or metagenome-assembled genomes (MAGs) (Chaumeil et al., 2019; Parks et al., 2015). Annotation was performed by Metascan (Cremers et al., 2022 under revision). The annotation method was described previously by in 't Zandt et al. (2020), Poghosyan et al. (2020). Briefly, genes were called by Prodigal (Hyatt et al., 2010) and subsequent open reading frames were annotated with HMMER (Eddy, 2009) and a set of custom-made databases.

DNA sequencing data from the slow-growing isolate Pslow were quality-checked and trimmed with BBDuk, assembled with MetaSpades and annotated with Metascan. The DNA sample consisted of two genomes (a very minor contaminant) so we separated the contigs using Maxbin 2.0. (Wu et al., 2015).

DNA Illumina reads from the fast-growing isolate Pfast were quality controlled and trimmed using BBDuk with minimum trim quality of 18 and length of 100. ONT reads were filtered to a minimum length of 3000 using BBtools utilities, and then were quality controlled and trimmed using Porechop (<https://github.com/rrwick/Porechop>) with minimum split read size of 3000. Illumina and ONT quality-trimmed reads were assembled using Unicycler with a minimum length of 1000 in the resulting. Metascan was used for annotation. Completion and contamination scores of the Pslow and Pfast assemblies were estimated using CheckM's lineage workflow. The whole-genome phylogenetic position of both assemblies was inferred using GTDB-tk. If not specified, settings were default.

### 2.4.3. Transcriptome analysis

The RNA reads were trimmed using Sickel and mapped with BBMap (allowing 1% mismatch, BBtools) to the protein-coding genes of each isolate or to the contigs of the whole metagenome. Then, transcripts per million (TPM) were calculated in Excel for each gene in each sample: first, reads per kilobase were calculated (read counts divided by the length of each gene in kilobases); second, the "per million" scaling factor was calculated (sum of all the reads per kilobase in one sample divided by one million); and third, TPM were calculated (reads per kilobase of each gene divided by the "per million" scaling factor). Approximately,

the top 10% most highly expressed genes in each microorganism or bin were considered as “highly-expressed”. The RNA coverage of each bin in the metagenome was calculated or defined as the number of bases mapped to the set of protein-coding genes from each bin divided by the total number of bases in each bin. Amidase sequences were retrieved by searching for “amidase”, “amidohydrolase”, and “amidotransferase” terms in the annotated metagenome. The highly-expressed and uncharacterized amidase sequences were aligned with Clustal Omega (Higgins and Sharp, 1988) and MUSCLE (Edgar, 2004) and the phylogenetic trees were created with MEGA7 (Kumar et al., 2016) and MEGA11 (Tamura et al., 2021) using the maximum likelihood algorithm (Jones et al., 1992) and bootstrap analysis or the neighbor-joining method to analyse the tree topology (Saitou and Nei, 1987).

### 3. Results and discussion

#### 3.1. Bioreactor performance and bacterial community changes

A bioreactor was inoculated with sludge from a WWTP treating hospital waste. APAP was added as the sole carbon source at all times during the experiment and it was fully removed since the beginning without lag phase. No transformation products were detected. To discard the possibility of abiotic removal such as adsorption to biomass, we measured APAP concentration in the presence of autoclaved sludge or active biomass used in the bioreactor inoculum. While active biomass removed 50 mg/L of APAP in 4 h, autoclaved biomass did not remove APAP during the four days of the experiment (Supplementary Fig. S1).

The microbial community was very diverse and changed during the different operational settings (Fig. 1). In the first start-up phase, the total suspended solids (TSS) gradually increased to about 1.1 g/L as all biomass was retained in the bioreactor via a membrane module. The HRT was 1.8 days. Under these conditions, the microbial community was dominated by members of the families *Chitinophagaceae*, *Halangiaceae*, *Phycisphaeraceae*, *Pseudomonadaceae*, *Saccharimonadaceae*, and *Sphingobacteriaceae* when compared to the inoculum mix. In the second phase, a SRT of 10 days was maintained in order to keep the biomass concentration (TSS) stable at a steady state. This led to a decrease of the relative abundance of *Pseudomonadaceae*, *Phycisphaeraceae*, and *Sphingobacteriaceae* while increasing *Burkholderiaceae*, *Chitinophagaceae*, and *Polyangiaceae*. In the third phase, the HRT was increased from 1.8 to 3.7 days resulting in a bacterial community dominated by the heterotrophic bacteria *Blastocatellaceae*, *Burkholderiaceae*, and *Chitinophagaceae*. *Nitrospiraceae* were also enriched which might be the result of growth on low concentration of residual ammonium in the reactor. Overall, the alpha diversity (richness and evenness of species) decreased over time in the bioreactor which corresponds to a selection and enrichment process (Supplementary Fig. S2). The previously mentioned taxa are normally found in WWTPs due to their ability

to degrade organic matter or ammonium/nitrite (*Nitrospira*) (Morin et al., 2020; Saunders et al., 2016). The presence of heterotrophs able to degrade complex organic matter (i.e. *Chitinophagaceae* and *Polyangiaceae*) might indicate possible predation and biomass recycling in the bioreactor (Petters et al., 2021). Furthermore, members of the *Pseudomonadaceae* and *Burkholderiaceae* families have been reported to degrade APAP and 4-AP, respectively (Park and Oh, 2020a; Takenaka et al., 2003; Žur et al., 2018a).

#### 3.2. Paracetamol degradation by two *Pseudomonas* spp. isolates

After serial dilutions of the bioreactor biomass, and plating the highest dilution showing APAP removal on agar mineral medium with APAP as sole carbon source, two *Pseudomonas* spp. were obtained (Fig. 1B (Batch) and Fig. 2). APAP medium without inoculum did not show APAP removal and both *Pseudomonas* isolates were not able to grow on synthetic medium without APAP. *Pseudomonas* sp. Pfast degraded 200 mg/L APAP in 10 h and converted it into 4-AP, which precipitated in the medium as a dark-brown solid. Since 4-AP was purchased as a white solid, we dissolved 4-AP in the bioreactor synthetic medium without bacteria and observed a color change in the medium and an abiotic removal due to precipitation (Supplementary Fig. S3). Kim et al. (2017) observed that HQ was a white solid, but the formation of a charge-transfer complex with quinone turned it into a dark solid. Therefore, 4-AP might also be forming complexes that lead to its coloration and precipitation. 4-AP might also be transformed by the Pfast isolate much slower than APAP. HQ was also detected as an intermediate but in a much lower concentration than 4-AP (data not shown). The other *Pseudomonas* sp., Pslow, degraded 200 mg/L APAP in approximately 90 d without the accumulation of aromatic transformation products. Since APAP was not degraded in the synthetic medium without bacteria and it did not adsorb to autoclaved sludge (Supplementary Fig. S1), we hypothesized that *Pseudomonas* Pslow cleaved the aromatic ring. If the ring cleavage is a slow reaction, this step might be coupled to the slow production of 4-AP after APAP amide cleavage. In the Pfast isolate, this process might be imbalanced because the formation of 4-AP is faster than the later ring cleavage reaction. Previous studies showed that other *Pseudomonas* spp. are also able to degrade APAP in a few hours (De Gussem et al., 2011; Hu et al., 2013; Park and Oh, 2020a; Zhang et al., 2013; Žur et al., 2018a). However, we are not aware of reports describing bacteria that degrade APAP at low rates.

#### 3.3. Highly-expressed amidases in the two *Pseudomonas* spp. isolates

After DNA and RNA sequencing, a highly expressed gene cluster was identified in the Pfast isolate that contained a putative amide transporter (AmiS/UreI family, OACKLNDA\_05759) and an amidase-like protein

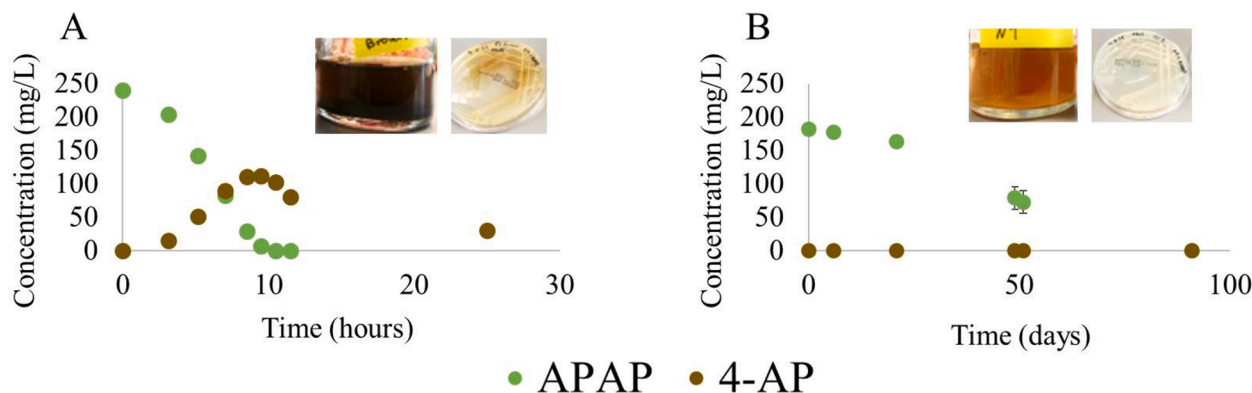


Fig. 2. APAP biodegradation rates of two *Pseudomonas* spp. isolated from the bioreactor by serial dilutions and plating. A corresponds to the fast-growing *Pseudomonas* sp. Pfast and B to the slow-growing *Pseudomonas* sp. Pslow. Abbreviations: APAP, paracetamol; 4-AP, 4-aminophenol.



(OACKLND\_05760) with 85% sequence identity to an aryl acylamidase known to convert APAP into 4-AP and acetate (Ko et al., 2010; Lee et al., 2015). The transporter might be catalyzing the uptake of APAP or the excretion of 4-AP. The genome of the Pslow isolate contained neither this amidase nor the putative amide transporter. Instead, it encoded three other amidases with  $\geq 95\%$  query coverage and 28–31% identity to the Pfast amidase. The most similar amidase (31% identity, BKDBLJDL\_05334) was upregulated in the transcriptome of strain Pslow cultivated with APAP as the sole carbon source. This amidase was encoded in a gene cluster together with a gene for a zinc-dependent hydrolase (BKDBLJDL\_05335). Interestingly, these genes were also present in the fast-growing *Pseudomonas* isolate, but not highly expressed. The difference in APAP biodegradation rate and consequently, growth between both *Pseudomonas* spp. was most likely related to the presence of OACKLND\_05760 amidase in Pfast, which might be able to transform APAP to 4-AP at high rates. Another option could be that the putative amide transporter OACKLND\_05759 was involved in a faster uptake of APAP and thus, transformation into 4-AP. Further studies are needed to answer this question.

The highly expressed amidase gene of strain Pslow was present in the chromosome of numerous *Pseudomonas* species registered in the NCBI nucleotide collection. However, the highly expressed amidase gene from strain Pfast was only found in a few microorganisms that came from various locations around the world (Australia, China, Pakistan, India, Korea, India, Poland): in the plasmid of multi-drug resistant *Acinetobacter* spp. isolated from patients and hospitals (Ghaly et al., 2020; Kizny Gordon et al., 2020; Zou et al., 2017); and in the chromosome of *Pseudomonas* and *Burkholderia* spp. isolated from soil, activated sludge, and hospitals (D'Souza et al., 2019; Ko et al., 2010; Patil et al., 2017; Zú et al., 2018b). Many bacteria contained a similar AmiS/UreI family transporter gene next to the amidase gene and different mobile genetic elements nearby (Tn3 transposons, IS630 insertion sequences and Int11 integrases). Our strain, Pfast, also had two insertion sequences (IS6100 and IS21, OACKLND\_05756, OACKLND\_05781), one Tn3 transposase gene (OACKLND\_05752), and one recombinase gene (OACKLND\_05755) near the highly-expressed amidase gene. Consequently, the whole gene cluster might have been exchanged between different species via horizontal gene transfer (HGT) (Rios Miguel et al., 2020). Finally, the low number of homologous proteins in the NCBI database might indicate the recent evolution of this amidase towards paracetamol biodegradation or our limited ability to find and identify these genes.

### 3.4. Amidase diversity in the metagenome

To check and confirm whether the bioreactor microbial community contained more unidentified amidases involved in APAP and

intermediate conversion, we analyzed the total metagenome at operational day 77. Before analyzing the amidase genes, 14 MAGs were recovered from the bioreactor metagenome and approximately 30% of the total reads remained unbinned. The binning process and taxonomy assignment is a required step before the analysis of genes of interest because it allows the linkage of these genes to a specific microbial genome from the metagenome. Table 1 shows the 14 recovered MAGs ordered from highest to lowest coverage based on RNA sequencing data (calculated with RNA bases mapped to protein-coding genes). *Chitinophagaceae* and *Myxococcales* were the most active (RNA coverage) bacteria and also the most abundant (DNA coverage) together with *Microbacterium* and *Patescibacteria*. Despite the high abundance of the *Patescibacteria* MAG, it had low completeness. The reason for this might be that the single copy genes normally used to calculate completeness are often not detected in *Patescibacteria* genomes (Brown et al., 2015). *Pseudomonas* spp. were low abundant in the metagenome and only present in the unbinned reads.

The highest BLAST identity match of the Pfast amidase was 50% for proteins encoded on the unbinned contigs. The 14 MAGs only contained amidases with a maximum of 30% sequence identity. For the Pslow isolate, the highest match was 50% for proteins encoded on the unbinned contigs as well as the *Rubrivivax* and *Betaproteobacteria* MAGs. Since the APAP concentration was below the detection limit ( $\sim 0.2$  mg/L) in the bioreactor, but continuously supplied with the medium inflow, uncharacterized amidases might be responsible for APAP biodegradation at low concentrations in the bioreactor.

A phylogenetic tree was created with the top 150 most expressed amidases in the metagenome, the uncharacterized amidases (enzymes annotated as “amidase” and whose function is not known) present in both *Pseudomonas* isolates, and five amidases known to degrade APAP obtained from literature and databases (Supplementary Fig. S4, Supplementary Table S1). All the uncharacterized amidases from the metagenome and the *Pseudomonas* isolate genomes clustered together (green cluster in Supplementary Fig. S4), including four amidases known to degrade paracetamol (Ko et al., 2010; Lee et al., 2015; Yun et al., 2017; Zhang et al., 201220202019). This group belongs to the Amidase Signature (AS) enzyme family [EC:3.5.1.4] characterized by a highly conserved signature region of approximately 160 amino acids that includes a canonical catalytic triad (Ser-cisSer-Lys) and a Gly/Ser-rich motif (GGSS[GS]G). One amidase (AGC74206.1 dimethoate hydrolase DmhA), previously reported to degrade APAP (Chen et al., 2016), did not cluster in this group (Supplementary Fig. S4). Consequently, there is the possibility that other amidase families are also able to transform APAP. For instance, a histone deacetylase-like amidohydrolase clustered together with the APAP-degrading amidase DmhA, suggesting its reactivity towards APAP.

The green AS amidase cluster of the phylogenetic tree in

**Table 1**

Metagenome-assembled genomes (MAGs) from the bioreactor at day 77. CheckM was used to check the quality of the MAGs. Taxonomy was assigned until the highest level possible using GTDB-Tk. RNA coverage is the average of three replicate samples while DNA coverage is based on one sample.

MAG (metaspades + das_tool)	Completeness (%)	Contamination (%)	Strain heterogeneity	Genome size (Mbp)	DNA coverage	RNA coverage $\pm$ SD
<i>Chitinophagaceae_2</i> ; g_Niabella	98.2	0.7	0.0	3.4	51.4	15.5 $\pm$ 4.2
<i>Myxococcales_1</i> ; g_Haliangium	87.1	3.3	0.0	7.5	21.3	15.3 $\pm$ 5.5
<i>Bacteroidetes</i> ; f_Sphingobacteriaceae	98.7	1.0	100.0	3.2	9.7	5.4 $\pm$ 1.8
<i>Chitinophagaceae_1</i> ; g_Niastella	98.3	2.7	77.8	3.0	10.7	3.7 $\pm$ 1.2
<i>Patescibacteria</i> ; f_Saccharimonadaceae	66.4	3.4	20.0	1.1	26.7	3.3 $\pm$ 0.2
<i>Microbacterium</i>	100.0	0.0	0.0	3.5	27.0	2.8 $\pm$ 1.1
<i>Acidobacteria</i>	97.4	3.7	0.0	4.7	11.1	2.1 $\pm$ 0.4
<i>Rubrivivax</i>	80.2	40.0	12.4	6.4	7.1	1.6 $\pm$ 0.5
<i>Myxococcales_2</i> ; g_Haliangium	77.4	6.3	30.0	10.3	8.1	1.4 $\pm$ 0.3
<i>Allicyclophilius denitrificans</i>	98.1	1.6	69.2	4.8	16.6	1.4 $\pm$ 0.4
<i>Chitinophagaceae_3</i> ; g_Niabella	76.1	1.0	20.0	3.1	4.6	1.3 $\pm$ 0.4
<i>Betaproteobacteria</i> ; o_Burkholderiales	95.7	11.4	75.0	4.9	20.1	1.1 $\pm$ 0.3
<i>Actinomycetales</i> ; g_Nocardioides	54.8	2.3	0.0	2.0	4.5	0.8 $\pm$ 0.5
<i>Comamonadaceae</i>	52.0	4.0	20.0	3.6	4.7	0.6 $\pm$ 0.2

Supplementary Fig. S4 was analyzed in more detail (Fig. 3). The amidase gene expression level in each bin/MAG was added to the tree (i.e. top 10%) and the amino acid sequences were manually blasted against the NCBI non-redundant protein database to improve the annotation. Furthermore, partial sequences like one highly-expressed amidase gene from *Betaproteobacteria* (EADEFLN\_03924) were removed from the analysis. Twelve amidases were identified as “Asp-tRNA(Asn)/Glu-tRNA(Gln) amidotransferase subunit GatA” and they all clustered together

(green cluster in Fig. 3). This type of amidase is involved in the transformation of Glu-tRNA<sup>Gln</sup> to Gln-tRNA<sup>Gln</sup> for the synthesis of proteins. Gene duplication and mutation events in this amidotransferase were probably the key contributors to the high number of uncharacterized amidases with broad substrate specificity.

Another cluster, with low bootstrap support, in the phylogenetic tree of Fig. 3 contained highly-expressed amidases (top 10%) of the *Pseudomonas* genomes and the *Microbacterium* MAG (red amidases in Fig. 3,

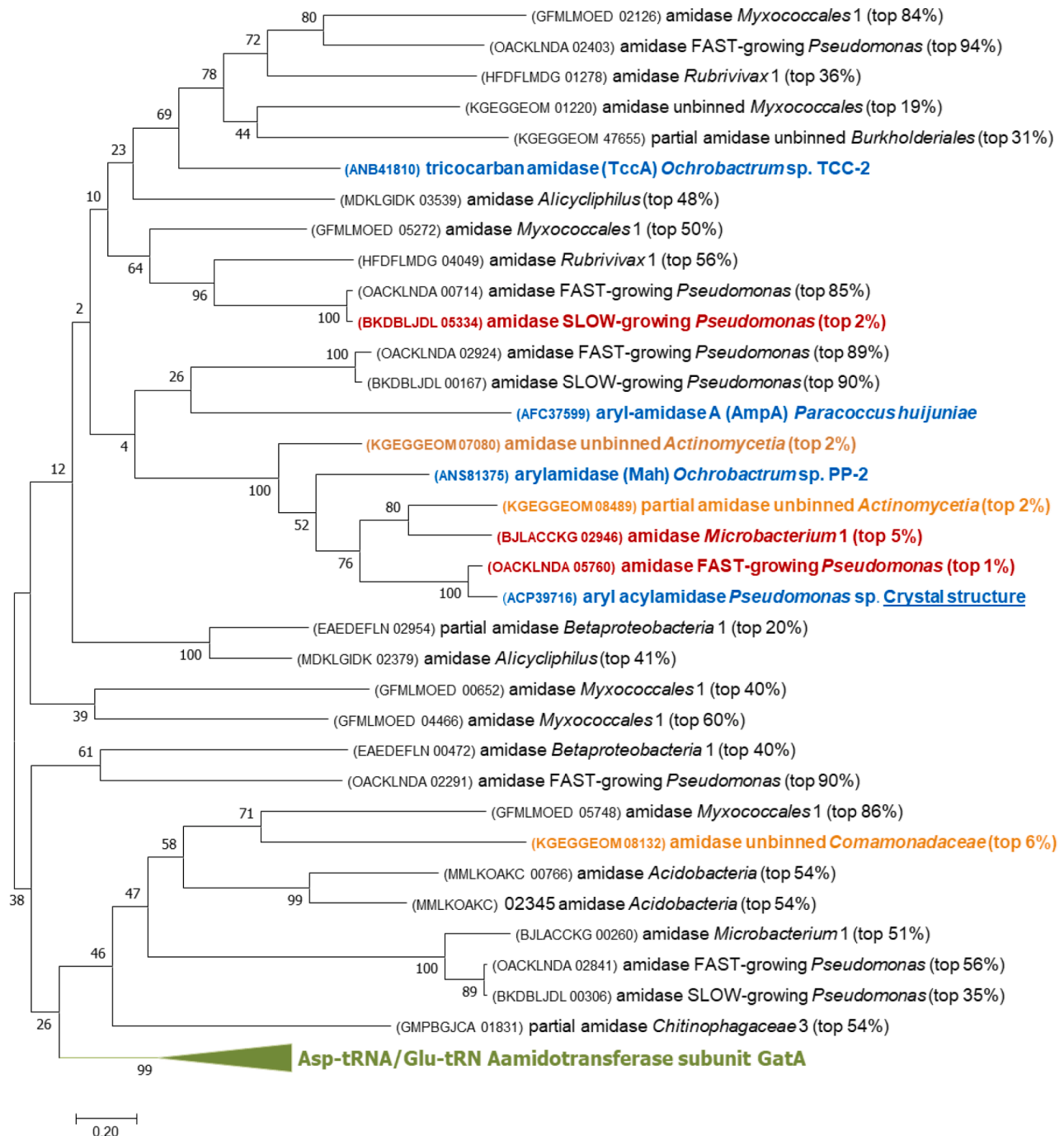


**Fig. 3.** Phylogenetic tree of the Amidase Signature (AS) enzyme family [EC:3.5.1.4] proteins in the bioreactor and the *Pseudomonas* isolates. The evolutionary history was inferred by using the Maximum Likelihood method (Jones et al., 1992). The tree with the highest log likelihood (-25739.55) is shown after bootstrapping 500 times. The percentage of trees in which the associated taxa clustered together is shown next to the branches. Evolutionary analyses were conducted in MEGA7 (Kumar et al., 2016). Amidases in blue are experimentally validated to degrade APAP. Amidases in red are the ones whose expression lies in the top 10% of all the genes in the *Pseudomonas* isolate transcriptomes, and the metatranscriptomes of the bioreactor mapping to a metagenome-assembled genome in this study. Orange amidases correspond to the amidase genes lying in the top 10% most expressed from the unbinning protein-coding genes. The green cluster corresponds to amidases annotated as the Asp-tRNA(Asn)/Glu-tRNA(Gln) amidotransferase subunit GatA.

OACKLND05760, BKDBLJDL05334, BJLACCKG\_02946). The *Microbacterium* amidase only had 91% query coverage and 63% identity to the closest amidase in the NCBI non-redundant protein database. This means that this amidase was sequenced for the first time and thus, the evolution of amidases towards paracetamol biodegradation might be an ongoing process. The *Microbacterium* amidase was part of a highly-expressed gene cluster containing a flavin reductase (BJLACCKG\_02944), an arylformamidase (BJLACCKG\_02945), a branched-chain amino acid ABC transporter (BJLACCKG\_02947, BJLACCKG\_02948, BJLACCKG\_02949, BJLACCKG\_02950, BJLACCKG\_02951), and one oxidoreductase (BJLACCKG\_02952). Furthermore, an IS110 family transposase gene (BJLACCKG\_02943) was right next to this highly expressed gene cluster. Four amidases known to degrade APAP were also part of the phylogenetic tree cluster containing the highly-expressed amidases of the *Pseudomonas* genomes and *Microbacterium* MAG (ANS81375.1 arylamidase Mah, ACP39716.2 aryl acylamidase, ANB41810.1 tricocarban amidase TccA, AFC37599.1 arylamidase A AmpA; blue amidases in Fig. 3). Three amidase genes present on the unbinned contigs were highly expressed in relation to all the unbinned protein-coding genes (top 10%, orange amidases in Fig. 3). They were affiliated with *Actinomycetia* and *Comamonadaceae* spp. (KGEKGGEOM\_07080, KGEKGGEOM\_08489, KGEKGGEOM\_08132) and might also be degrading APAP in the bioreactor. Non-highly-expressed amidase genes might also have the potential to degrade APAP even though their genes were not strongly regulated when APAP was present. For instance, the non-highly-expressed amidase OACKLND00714 of the Pfast strain was identical to the highly-expressed amidase BKDBLJDL\_05334 of the Pslow strain, so it had the potential to degrade APAP at slow rates but it was not highly-expressed in Pfast.

Finally, a multiple sequence alignment was performed with the amidases known to degrade APAP (except for DmhA which is not part of the AS family) and the highly expressed amidases from the *Pseudomonas* genomes and the metagenome (Supplementary File 2). Lee et al.

previously determined the three-dimensional structure of the amidase ACP39716.2 with APAP as a substrate (Lee et al., 2015). They revealed several residues involved in catalysis and APAP binding that we investigated in our alignment. The aligned amidases contained a conserved catalytic triad (Ser<sup>187</sup>-cisSer<sup>163</sup>-Lys<sup>84</sup>, highlighted in green), Gly/Ser-rich motif (GGSSGG, in bold) and oxyanion hole ([G]GGs, in bold). The substrate-binding pocket contained two loop regions (highlighted in fair and dark grey) and one  $\alpha$ -helix (highlighted in blue) that were less conserved. In the crystal structure of ACP39716, another two residues (Tyr<sup>136</sup> and Thr<sup>330</sup>, highlighted in yellow) were described to bind to the hydroxyl group at the para-position in APAP via hydrogen bonds with two water molecules. However, Thr<sup>330</sup> was only present in approximately half of the aligned amidase sequences and Tyr<sup>136</sup> was not present in any of them. Thus, the amidases from this study might have different substrate specificities compared to the ACP39716.2 amidase. Furthermore, we conclude that Tyr<sup>136</sup> and Thr<sup>330</sup> are not strictly necessary for APAP binding and degradation.

### 3.5. Paracetamol-degradation pathway: highly-expressed gene candidates

The first step in APAP biodegradation is the cleavage of the amide bond by an amidase to produce 4-AP and acetate (Fig. 4). In each *Pseudomonas* genome, a different highly expressed amidase was identified presumably performing this cleavage (OACKLND05760, BKDBLJDL05334). In the bioreactor metagenome, the *Microbacterium* MAG was the only one with a highly expressed amidase inside the AS family cluster (BJLACCKG\_02946), from which four amidases were previously reported to degrade APAP (Fig. 3). The *Betaproteobacteria* MAG also had a highly expressed uncharacterized amidase gene (EAE-DEFLN\_03924). However, the nucleotide sequence was partial so we could not check its classification. Therefore, *Microbacterium* (and *Betaproteobacteria*) might have been involved in transforming APAP into 4-AP together with some low abundant bacteria in the unbinned group.

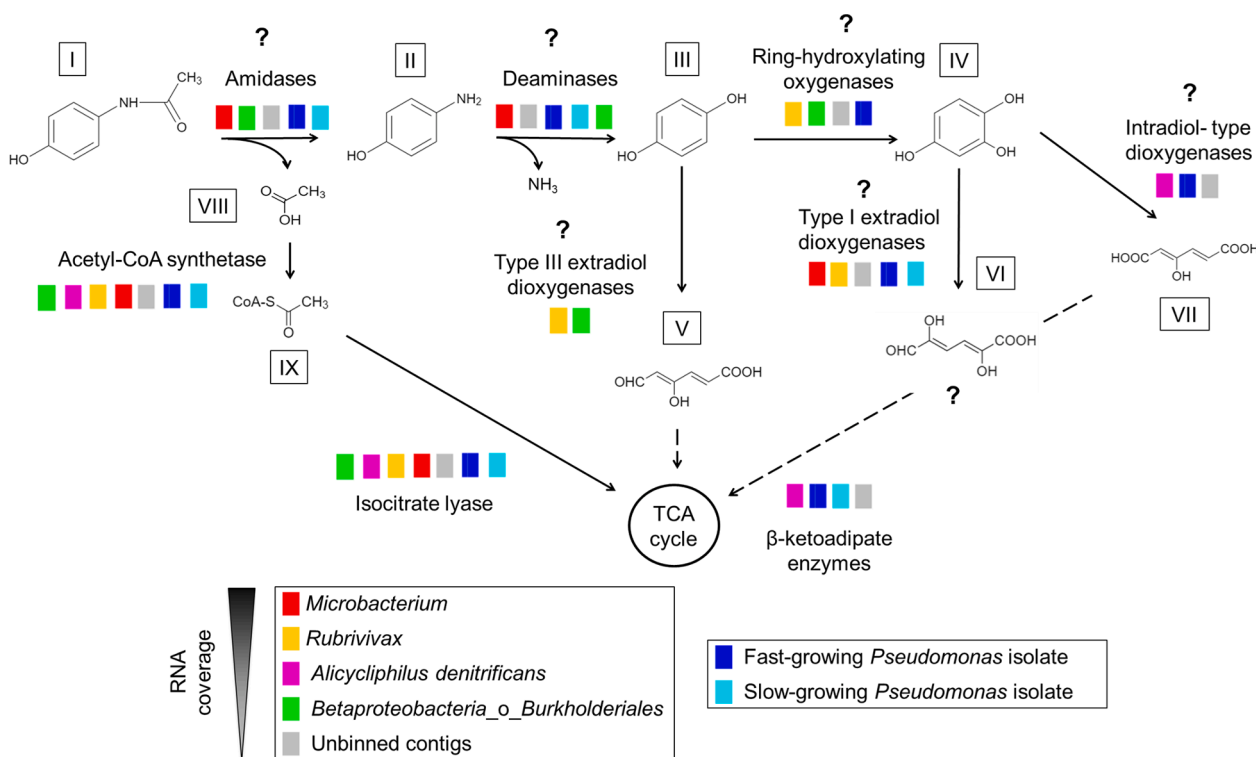


**Fig. 4.** Paracetamol degradation pathway by the bioreactor microbial community and the *Pseudomonas* isolates. The question marks represent candidate enzymes and metabolites. Dashed lines correspond to conversions requiring more than one step. I paracetamol; II 4-aminophenol; III hydroquinone; IV hydroxyquinone or 1,2,4-trihydroxybenzene; V 4-hydroxy-6-oxo-2,4-hexadienoic acid; VI 2,5-dihydroxy-6-oxo-2,4-hexadienoic acid; VII 3-hydroxy-cis, cis-muconate or 3-hydroxy-2,4-hexadienedioic acid; VIII acetate; IX acetyl-CoA; TCA tricarboxylic acid.

An alternative first step for APAP biodegradation could be its hydroxylation to form 3-hydroxyacetaminophen, a metabolite measured in soil by Li et al. (2014). However, due to the high concentration of 4-AP in the *Pseudomonas* experiments, the cleavage of the amide bond might be the dominant mechanism.

The enzyme deaminating 4-AP is still unknown and we did not find an obvious gene responsible for this reaction. Uncharacterized Rida family protein genes were highly expressed in the two *Pseudomonas* genomes and in the *Microbacterium* and *Betaproteobacteria* MAGs (OACKLND\_05815, OACKLND\_03065, BKDBLJDL\_03266, BKDBLJDL\_01320, BJLACCKG\_02940, BJLACCKG\_02936, EAEDEFLN\_02051). Therefore, these proteins might have been involved in deaminating 4-AP or deaminating the aminomuconate intermediates after ring cleavage (He and Spain, 1998). Furthermore, two ammonia-lyase genes were highly expressed in the genome of the Pslow strain: aspartate ammonia-lyase and ethanolamine ammonia-lyase (BKDBLJDL\_01355, BKDBLJDL\_02838). However, these genes were not highly expressed in the Pfast genome and the metagenome from the bioreactor.

The investigated bacteria did not use any known hydroquinone 1,2-dioxygenase, which is a type III ring-cleaving extradiol dioxygenase (cupin superfamily) with a catalytic mechanism analogous to that of the extradiol-type dioxygenases. Instead, the up-regulated type III extradiol dioxygenase genes present in bioreactor MAGs (*Chitinophagaceae*\_1,2 and *Betaproteobacteria*: 3-hydroxyanthranilate 3,4-dioxygenase (NLCKOFOF\_01117, JPNLMFAJ\_02227, EAEDEFLN\_00964); *Bacteroidetes*, *Rubrivivax*, and *Myxococcales*\_2: homogentisate 1,2-dioxygenase (KGBAGMN\_02738, HFDFLMDG\_05905, OPIJCCOK\_08966)) might have cleaved the aromatic ring of HQ to produce 4-hydroxymuconic semialdehyde as previously described (Žur et al., 2018b) (Fig. 4). Homogentisate 1,2-dioxygenase and 3-hydroxyanthranilate 3,4-dioxygenase are type III extradiol dioxygenases able to cleave the aromatic ring of non-catecholic substrates, which are characterized by not having vicinal diols. For example, (homo)gentisate and hydroquinone have two hydroxyl groups in *para* position and 3-hydroxyanthranilate has one hydroxyl, one amino, and one carboxylic acid group as ring substituents. These two dioxygenases are involved in the degradation of aromatic amino acids. Therefore, bacteria might use the side activities of existing enzymes to degrade aromatic micropollutants such as APAP.

The ring cleavage of aromatic compounds containing hydroxyl and amino substituents (i.e. 2-aminophenol, 3-hydroxyanthranilate, and 5-aminosalicylate) has been previously reported (Hintner et al., 2004; Li de et al., 2013; Takenaka et al., 1997; Wang et al., 2020). Therefore, the aromatic ring of 4-AP might also be cleaved before deamination by class III ring-cleaving dioxygenases. However, metabolites confirming this pathway have not yet been measured.

An alternative route for the direct ring cleavage of HQ is the hydroxylation of HQ to form hydroxyquinol (1,2,4-trihydroxybenzene) and later, the ring cleavage of hydroxyquinol by an intradiol-type dioxygenase (Ferraroni et al., 2005; Takenaka et al., 2003) or an extradiol-type dioxygenase, probably from the vicinal oxygen chelate (VOC) or type I superfamily (Murakami et al., 1999) (Fig. 4). Catechol has been previously measured during APAP microbial degradation (Dai et al., 2021; Ivshina et al., 2005) suggesting that it could be a transformation product that is further cleaved by intradiol-type or extradiol-type dioxygenases. The hydroxylation of HQ can be performed by ring-hydroxylating dioxygenases or monooxygenases. In the Pfast isolate genome, an uncharacterized ring-hydroxylating dioxygenase (OACKLND\_03401) and an intradiol catechol 1,2-dioxygenase (OACKLND\_05722) were highly expressed. Furthermore, two uncharacterized extradiol-type dioxygenases were highly expressed in both *Pseudomonas* isolate genomes (OACKLND\_01459, BKDBLJDL\_01807). These dioxygenases were similar to 4,5-DOPA dioxygenase, which is part of the VOC extradiol dioxygenases (Wang et al., 2019). In the bioreactor, the *Rubrivivax* MAG had a phenol hydroxylase (HFDFLMDG\_03468, HFDFLMDG\_03467, HFDFLMDG\_03466), an

uncharacterized ring-hydroxylating dioxygenase (HFDFLMDG\_03024), a 4-hydroxybenzoate 3-monooxygenase (HFDFLMDG\_05635), and an extradiol protocatechuate 4,5-dioxygenase (HFDFLMDG\_01086, HFDFLMDG\_01087) highly expressed. The *Microbacterium* MAG contained a highly-expressed VOC extradiol 3,4-dihydroxyphenylacetate (homoprotocatechuate) 2,3-dioxygenase involved in the degradation of tyrosine (BJLACCKG\_03009). The *Betaproteobacteria* MAG had a putative ring hydroxylating dioxygenase (EAEDEFLN\_00364), and a 4-hydroxyphenylpyruvate dioxygenase (EAEDEFLN\_02889) able to hydroxylate and decarboxylate aromatic rings in the tyrosine degradation pathway. Many other MAGs contained this gene up-regulated, i.e. *Bacteroidetes*, *Comamonadaceae* and *Myxococcales*\_2 (KGBAGMN\_02075, JMGBCLMB\_02041, OPIJCCOK\_08967). Finally, the *Alicyclophilus* MAG had a highly expressed gene cluster containing an MFS transporter (MDKLIDK\_02282), a tripartite tricarboxylate transporter substrate binding protein (MDKLIDK\_02283), an muconolactone D-isomerase (MDKLIDK\_02284), an 3-oxoadipate enol-lactonase (MDKLIDK\_02285), a 1,6-dihydroxycyclohexa-2,4-diene-1-carboxylate dehydrogenase (MDKLIDK\_02286), an intradiol catechol 1,2-dioxygenase gene (MDKLIDK\_02287), and a muconate cycloisomerase (MDKLIDK\_02288). This highly-expressed gene cluster suggests the ability of *Alicyclophilus* to fully degrade hydroxyquinol via the oxoadipate pathway. Interestingly, the *Alicyclophilus* MAG had hydroquinone dioxygenase genes (MDKLIDK\_00653, MDKLIDK\_00654) that were not highly expressed.

Acetyl-CoA synthetase genes and genes encoding enzymes involved in the tricarboxylic acid (TCA) and glyoxylate cycles (isocitrate lyase) were highly expressed in the transcriptome of both *Pseudomonas* spp. and several MAGs (i.e. *Microbacterium*, *Rubrivivax*, *Alicyclophilus*, and *Actinomycetales*), thus indicating their ability to grow on acetate after cleaving the APAP amide bond or via cross-feeding from other bacteria (Fig. 4). Finally, the highly-expressed gene encoding an uncharacterized carboxymuconolactone decarboxylase family protein could be involved in the conversion of muconolactone intermediates to eventually reach the TCA cycle for bacterial growth in the *Pseudomonas* isolates (OACKLND\_03472, BKDBLJDL\_01962). The *Microbacterium*, *Rubrivivax*, and *Betaproteobacteria* MAGs had highly-expressed dioxygenases but they did not have up-regulated genes belonging to the  $\beta$ -ketoadipate pathway, involved in the conversion of aromatic metabolites into TCA intermediates. Therefore, it is unclear whether they were able to assimilate aromatic compounds or not. Furthermore, the *Rubrivivax* and *Alicyclophilus* MAGs did not have any highly-expressed amidase from the AS family suggesting that cross-feeding of acetate and aromatic intermediates was happening in the bioreactor.

The *Myxococcales* family is known for its diverse metabolism and its predatory nature, so the two bioreactor MAGs affiliated to the *Myxococcales* family might have lived from the metabolites and cellular components of decaying microorganisms (Müller et al., 2016). Similarly, the *Chitinophagaceae* family is known to degrade complex organic matter and therefore, the three bioreactor MAGs affiliated to the *Chitinophagaceae* family could also have been biomass recyclers in the bioreactor (Morin et al., 2020). The highest expressed metabolic genes of these MAGs were involved in the TCA cycle, gluconeogenesis, and metabolism of lipids, peptidoglycan, nucleotides, and amino acids, thus not providing many hints about their exact catabolism or energy source. Similarly, the metabolism of *Bacteroidetes*, *Acidobacteria*, *Actinomycetales*, and *Comamonadaceae* MAGs was ambiguous and they might also be predators or biomass recyclers. In addition, we found that type II and type IV secretion systems were highly expressed in several MAGs (i.e. *Acidobacteria*, *Comamonadaceae*) which might have been involved in predation, defense, and conjugation activities between microorganisms (Aharon et al., 2021; Sgro et al., 2019). However, some of these MAGs might also degrade APAP transformation products via their highly-expressed dioxygenases (i.e. *Chitinophagaceae*\_1,2, *Bacteroidetes*, *Myxococcales*\_2). The *Patescibacteria* MAG mostly contained genes encoding carbohydrate degrading enzymes, so it might have thrived in



symbiosis with other microbial community members that produced exopolysaccharides.

### 3.6. Highly-expressed nitrification and denitrification genes in the bioreactor

The majority of the MAGs, except for *Patescibacteria* and *Myxococcales\_1*, had highly expressed genes encoding enzymes from the denitrification pathway. All four genes encoding the full pathway of denitrification could only be found in one MAG, affiliated with *Alicyclophilus denitrificans*, as well as the in the unbinned contigs: nitrate reductase, nitrite reductase, nitric oxide reductase, and nitrous oxide reductase. The bioreactor was fully aerated, but biomass was spatially organized in small granules (Supplementary Fig. S5), so there might have been anoxic conditions towards the inside of the granules favoring denitrification. Nitrate and nitrite were not added to the medium, so nitrifying microorganisms were apparently also active in the bioreactor. A single highly expressed ammonia monooxygenase (subunits A, B, C; KEGGGEOM\_12202, KEGGGEOM\_12201, KEGGGEOM\_12203) was encoded in the unbinned contigs, and affiliated with the complete ammonia oxidizer (comammox) *Nitrospira* sp. This finding suggests that some ammonia released from decaying biomass, from the paracetamol degradation and from the ammonia supply in the medium intended for assimilation (~1 mM) was converted into nitrate by comammox *Nitrospira* sp. and subsequently available for (oxygen-limited) denitrification.

## 4. Conclusions

On the basis of our cultivation and metagenomic analysis, we conclude that APAP was immediately degraded by the activated sludge of a hospital WWTP and that a diverse microbial community was enriched under low APAP concentrations in a membrane bioreactor. High APAP concentrations in batch led to the dominance of a fast-growing *Pseudomonas* species. Several uncharacterized amidases from the AS family were highly expressed in the genome of a fast- and a slow-growing *Pseudomonas* species and the bioreactor metagenome. They might be cleaving APAP into 4-AP at different rates. Genes encoding for uncharacterized RidA family proteins were highly expressed in the genome of the *Pseudomonas* isolates and several bioreactor MAGs. They are known to have deaminase activity, so they might be converting 4-AP to HQ or cleaving reactive enamine intermediates. Genes encoding for intradiol- and extradiol-type dioxygenases were highly expressed in the genomes of the *Pseudomonas* isolates and the bioreactor metagenome. Many of these genes are part of the degradation pathway of aromatic amino acids. Therefore, microorganisms might take advantage of the side activities of existing enzymes encoded in their genomes for the degradation of APAP transformation products. Candidate APAP-degrading amidases, deaminases, and dioxygenases were not combined in the same gene cluster. Highly expressed genes encoding amidases were often found in the vicinity of mobile genetic elements, which suggests that APAP-degrading amidase genes are currently being exchanged between different bacteria via HGT.

Taken together, these results suggest a role of uncharacterized amidases, deaminases and dioxygenases in the biodegradation of APAP and the use of cross-feeding to efficiently degrade APAP in WWTP microbial communities. Furthermore, the high number of microorganisms able to degrade APAP might be the result of the broad substrate spectrum of amidases and its evolution, together with the fact that just one enzyme (amidase) is needed to grow on APAP-derived acetate. This study contributes to a better understanding of microbial evolution towards pharmaceutical biodegradation and demonstrates the complexity of this process due to the broad substrate spectrum of the involved enzymes.

### Author contributions

ARM, MJ, HODC, and CW contributed to the conceptual framework

of the manuscript. ARM conducted the experiments and data analysis. GS, GC, and HODC contributed to bioinformatics analyses. TvA performed DNA and RNA Illumina sequencing of the slow-growing *Pseudomonas*. ARM wrote the manuscript with input from all the authors.

### Data Availability

All raw sequencing data (DNA and RNA) have been deposited at the read sequence archive (SRA) database of the NCBI under the BioProject ID PRJNA831879. The amino acid sequences and annotation of all genes in the metagenome and the *Pseudomonas* spp. genomes are deposited in Dans Easy (<https://doi.org/10.17026/dans-xwd-fbj5>). This dataset also contains the TPMs of the bioreactor and the *Pseudomonas* spp. transcriptomes and the amino acid sequences of the amidase genes used to create the phylogenetic trees in Fig. 3 and Supplementary Fig. S4.

### Declaration of Competing Interest

The authors declare that they have no known competing financial interests or personal relationships that could have appeared to influence the work reported in this paper.

### Acknowledgments

The authors thank Stefan Hertel and Erwin Koetse for letting us take sludge from the MBR and GAC of Pharmafilter. We also thank Rob de Graaf for sharing his expertise with the HPLC and Guylaine Nuijten for her help with bioreactors. This research was supported by NWO-TTW grant 15759 and NWO/OCW grant SIAM 024002002.

### Supplementary materials

Supplementary material associated with this article can be found, in the online version, at doi:[10.1016/j.wroa.2022.100152](https://doi.org/10.1016/j.wroa.2022.100152).

## References

- Aharon, E., Mookherjee, A., Pérez-Montaña, F., Mateus da Silva, G., Sathyamoorthy, R., Burdman, S., Jurkevitch, E., 2021. Secretion systems play a critical role in resistance to predation by *Bdellovibrio bacteriovorus*. *Res. Microbiol.* 172 (7), 103878.
- Alneberg, J., Bjarnason, B.S., de Bruijn, I., Schirmer, M., Quick, J., Ijaz, U.Z., Lahti, L., Loman, N.J., Andersson, A.F., Quince, C., 2014. Binning metagenomic contigs by coverage and composition. *Nat. Methods* 11 (11), 1144–1146.
- Brown, C.T., Hug, L.A., Thomas, B.C., Sharon, I., Castelle, C.J., Singh, A., Wilkins, M.J., Wrighton, K.C., Williams, K.H., Banfield, J.F., 2015. Unusual biology across a group comprising more than 15% of domain bacteria. *Nature* 523 (7559), 208–211.
- Callahan, B.J., McMurdie, P.J., Rosen, M.J., Han, A.W., Johnson, A.J.A., Holmes, S.P., 2016. DADA2: high-resolution sample inference from Illumina amplicon data. *Nat. Methods* 13 (7), 581–583.
- Chaumeil, P.A., Mussig, A.J., Hugenholtz, P., Parks, D.H., 2019. GTDB-Tk: a toolkit to classify genomes with the genome taxonomy database. *Bioinformatics* 36 (6), 1925–1927.
- Chen, Q., Chen, K., Ni, H., Zhuang, W., Wang, H., Zhu, J., He, Q., He, J., 2016. A novel amidohydrolase (DmhA) from *Sphingomonas* sp. that can hydrolyze the organophosphorus pesticide dimethoate to dimethoate carboxylic acid and methylamine. *Biotechnol. Lett.* 38 (4), 703–710.
- Cremers, G., Jetten, M.S.M., Op den Camp, H.J.M., Lückner, S., 2022. Metascan: METabolic analysis, SCreening and annotation of metagenomes. *Front. Bioinform.* 2, 861505.
- D'Souza, A.W., Potter, R.F., Wallace, M., Shupe, A., Patel, S., Sun, X., Gul, D., Kwon, J.H., Andleeb, S., Burnham, C.A.D., Dantas, G., 2019. Spatiotemporal dynamics of multidrug resistant bacteria on intensive care unit surfaces. *Nat. Commun.* 10 (1), 4569.
- De Gussem, B., Vanhaecke, L., Verstraete, W., Boon, N., 2011. Degradation of acetaminophen by *Delftia tsuruhatensis* and *Pseudomonas aeruginosa* in a membrane bioreactor. *Water Res.* 45 (4), 1829–1837.
- Grignat, R.D.S., Barros, M.G.A., Panatta, A.A.S., Bernal, S.P.F., Ottoni, J.R., Passarini, M. R.Z., Gonçalves, C.C.S., 2022. Medicines as an emergent contaminant: the review of microbial biodegradation potential. *Folia Microbiol. (Praha)*.
- Eddy, S.R., 2009. A new generation of homology search tools based on probabilistic inference. *Genome Inform.* 23 (1), 205–211.
- Edgar, R.C., 2004. MUSCLE: a multiple sequence alignment method with reduced time and space complexity. *BMC Bioinf.* 5 (1), 113.
- Ferraroni, M., Seifert, J., Travkin, V.M., Thiel, M., Kaschabek, S., Scozzafava, A., Golovleva, L., Schlömann, M., Briganti, F., 2005. Crystal structure of the

- hydroxyquinol 1,2-dioxygenase from nocardioideis simplex 3E, a key enzyme involved in polychlorinated aromatics biodegradation\*. J. Biol. Chem. 280 (22), 21144–21154.
- Gavrilescu, M., Demnerová, K., Aamand, J., Agathos, S., Fava, F., 2015. Emerging pollutants in the environment: present and future challenges in biomonitoring, ecological risks and bioremediation. New Biotechnol. 32 (1), 147–156.
- Ghaly, T.M., Paulsen, I.T., Sajjad, A., Tett, S.G., Gillings, M.R., 2020. A novel family of acinetobacter mega-plasmids are disseminating multi-drug resistance across the globe while acquiring location-specific accessory genes. Front. Microbiol. 11.
- Graham, E.D., Heidelberg, J.F., Tully, B.J., 2017. BinSanity: unsupervised clustering of environmental microbial assemblies using coverage and affinity propagation. PeerJ 5, e3035.
- Hart, A., Orr, D.L.J., 1974. Degradation of paracetamol by a *Penicillium* species. J. Pharm. Pharmacol. 26, 70P–71P. Supplement\_1.
- He, Z., Spain, J.C., 1998. A novel 2-aminomuconate deaminase in the nitrobenzene degradation pathway of *Pseudomonas pseudoalcaligenes* JS45. J. Bacteriol. 180 (9), 2502–2506.
- Higgins, D.G., Sharp, P.M., 1988. CLUSTAL: a package for performing multiple sequence alignment on a microcomputer. Gene 73 (1), 237–244.
- Hintner, J.P., Reemtsma, T., Stolz, A., 2004. Biochemical and molecular characterization of a ring fission dioxygenase with the ability to oxidize (substituted) salicylate(s) from *Pseudaminobacter salicylatoxidans*. J. Biol. Chem. 279 (36), 37250–37260.
- Hu, J., Zhang, L.L., Chen, J.M., Liu, Y., 2013. Degradation of paracetamol by *Pseudomonas aeruginosa* strain HJ1012. J. Environ. Sci. Health Part A 48 (7), 791–799.
- Hyatt, D., Chen, G.-L., LoCascio, P.F., Land, M.L., Larimer, F.W., Hauser, L.J., 2010. Prodigal: prokaryotic gene recognition and translation initiation site identification. BMC Bioinform. 11 (1), 119.
- in 't Zandt, M.H., Frank, J., Yilmaz, P., Cremers, G., Jetten, M.S.M., Welte, C.U., 2020. Long-term enriched methanogenic communities from thermokarst lake sediments show species-specific responses to warming. FEMS Microbes 1 (1).
- Jones, D.T., Taylor, W.R., Thornton, J.M., 1992. The rapid generation of mutation data matrices from protein sequences. Comput. Appl. Biosci. 8 (3), 275–282.
- Kanama, K.M., Daso, A.P., Mpenyana-Monyatsi, L., Coetzee, M.A.A., 2018. Assessment of pharmaceuticals, personal care products, and hormones in wastewater treatment plants receiving inflows from health facilities in North West Province, South Africa. J. Toxicol., 3751930.
- Kang, D.D., Li, F., Kirton, E., Thomas, A., Egan, R., An, H., Wang, Z., 2019. MetaBAT 2: an adaptive binning algorithm for robust and efficient genome reconstruction from metagenome assemblies. PeerJ 7, e7359.
- Kim, B., Storch, G., Banerjee, G., Mercado, B.Q., Castillo-Lora, J., Brudvig, G.W., Mayer, J.M., Miller, S.J., 2017. Stereodynamic quinone-hydroquinone molecules that enantioselectively convert 3-pyridyl-carbon via redox-interconversion. J. Am. Chem. Soc. 139 (42), 15239–15244.
- Kizny Gordon, A., Phan, H.T.T., Lipworth, S.I., Cheong, E., Gottlieb, T., George, S., Peto, T.E.A., Mathers, A.J., Walker, A.S., Crook, D.W., Stoesser, N., 2020. Genomic dynamics of species and mobile genetic elements in a prolonged blaIMP-4-associated carbapenemase outbreak in an Australian hospital. J. Antimicrobial. Chemother. 75 (4), 873–882.
- Klindworth, A., Pruesse, E., Schweer, T., Peplies, J., Quast, C., Horn, M., Glöckner, F.O., 2013. Evaluation of general 16S ribosomal RNA gene PCR primers for classical and next-generation sequencing-based diversity studies. Nucl. Acids Res. 41 (1), e1.
- Ko, H.J., Lee, E.W., Bang, W.G., Lee, C.K., Kim, K.H., Choi, I.G., 2010. Molecular characterization of a novel bacterial aryl acylamidase belonging to the amidase signature enzyme family. Mol. Cells 29 (5), 485–492.
- Kumar, S., Stecher, G., Tamura, K., 2016. MEGA7: molecular evolutionary genetics analysis version 7.0 for bigger datasets. Mol. Biol. Evol. 33 (7), 1870–1874.
- Lee, S., Park, E.H., Ko, H.J., Bang, W.G., Kim, H.Y., Kim, K.H., Choi, I.G., 2015. Crystal structure analysis of a bacterial aryl acylamidase belonging to the amidase signature enzyme family. Biochem. Biophys. Res. Commun. 467 (2), 268–274.
- Li de, F., Zhang, J.Y., Hou, Y.J., Liu, L., Hu, Y., Liu, S.J., Wang da, C., Liu, W., 2013. Structures of aminophenol dioxygenase in complex with intermediate, product and inhibitor. Acta Crystallogr. D Biol. Crystallogr. 69, 32–43. Pt 1.
- McMurdie, P.J., Holmes, S., 2013. phyloseq: an R package for reproducible interactive analysis and graphics of microbiome census data. PLoS One 8 (4), e61217.
- Morin, L., Goubet, A., Madigou, C., Pernelle, J.J., Palmier, K., Labadie, K., Lemaître, A., Michot, O., Astoul, L., Barbier, P., Almayrac, J.L., Sghir, A., 2020. Colonization kinetics and implantation follow-up of the sewage microbiome in an urban wastewater treatment plant. Sci. Rep. 10 (1), 11634.
- Müller, S., Strack, S.N., Ryan, S.E., Shawgo, M., Walling, A., Harris, S., Chambers, C., Boddicker, J., Kirby, J.R., 2016. Identification of functions affecting predator-prey interactions between *Myxococcus Xanthus* and *Bacillus subtilis*. J. Bacteriol. 198 (24), 3335–3344.
- Murakami, S., Okuno, T., Matsumura, E., Takenaka, S., Shinke, R., Aoki, K., 1999. Cloning of a gene encoding hydroxyquinol 1,2-dioxygenase that catalyzes both intradiol and extradiol ring cleavage of catechol. Biosci. Biotechnol. Biochem. 63 (5), 859–865.
- Nurk, S., Meleshko, D., Korobeynikov, A., Pevzner, P.A., 2017. metaSPAdes: a new versatile metagenomic assembler. Genome Res. 27 (5), 824–834.
- Palma, T.L., Donaldben, M.N., Costa, M.C., Carlier, J.D., 2018. Putative role of flavobacterium, dokdonella and methylphilus strains in paracetamol biodegradation. Water Air Soil Pollut. 229 (6), 200.
- Park, S., Oh, S., 2020a. Activated sludge-degrading analgesic drug acetaminophen: acclimation, microbial community dynamics, degradation characteristics, and bioaugmentation potential. Water Res. 182, 115957.
- Park, S., Oh, S., 2020b. Detoxification and bioaugmentation potential for acetaminophen and its derivatives using *Ensifer* sp. isolated from activated sludge. Chemosphere 260, 127532.
- Parks, D.H., Imelfort, M., Skennerton, C.T., Hugenholtz, P., Tyson, G.W., 2015. CheckM: assessing the quality of microbial genomes recovered from isolates, single cells, and metagenomes. Genome Res. 25 (7), 1043–1055.
- Patil, P.P., Mali, S., Midha, S., Gautam, V., Dash, L., Kumar, S., Shastri, J., Singhal, L., Patil, P.B., 2017. Genomics reveals a unique clone of *Burkholderia cenocepacia* harboring an actively excising novel genomic island. Front. Microbiol. 8.
- Petters, S., Groß, V., Söllinger, A., Pichler, M., Reinhard, A., Bengtsson, M.M., Ulrich, T., 2021. The soil microbial food web revisited: predatory myxobacteria as keystone taxa? ISME J. 15 (9), 2665–2675.
- Poghossyan, L., Koch, H., Frank, J., van Kessel, M.A.H.J., Cremers, G., van Alen, T., Jetten, M.S.M., Op den Camp, H.J.M., Lückner, S., 2020. Metagenomic profiling of ammonia- and methane-oxidizing microorganisms in two sequential rapid sand filters. Water Res. 185, 116288.
- Rios-Miguel, A.B., Jetten, M.S.M., Welte, C.U., 2021. Effect of concentration and hydraulic reaction time on the removal of pharmaceutical compounds in a membrane bioreactor inoculated with activated sludge. Microb. Biotechnol. 14 (4), 1707–1721.
- Rios Miguel, A.B., Jetten, M.S.M., Welte, C.U., 2020. The role of mobile genetic elements in organic micropollutant degradation during biological wastewater treatment. Water Res. X 9, 100065.
- Saitou, N., Nei, M., 1987. The neighbor-joining method: a new method for reconstructing phylogenetic trees. Mol. Biol. Evol. 4 (4), 406–425.
- Saunders, A.M., Albertsen, M., Vollertsen, J., Nielsen, P.H., 2016. The activated sludge ecosystem contains a core community of abundant organisms. ISME J. 10 (1), 11–20.
- Sgro, G.G., Oka, G.U., Souza, D.P., Cenens, W., Bayer-Santos, E., Matsuyama, B.Y., Bueno, N.F., dos Santos, T.R., Alvarez-Martinez, C.E., Salinas, R.K., Farah, C.S., 2019. Bacteria-killing type IV secretion systems. Front. Microbiol. 10.
- Siebert, C.M.K., Probst, A.J., Sharrar, A., Thomas, B.C., Hess, M., Tringe, S.G., Banfield, J. F., 2018. Recovery of genomes from metagenomes via a dereplication, aggregation and scoring strategy. Nat. Microbiol. 3 (7), 836–843.
- Takenaka, S., Murakami, S., Shinke, R., Hatakeyama, K., Yukawa, H., Aoki, K., 1997. Novel genes encoding 2-aminophenol 1,6-dioxygenase from *Pseudomonas* species AP-3 growing on 2-aminophenol and catalytic properties of the purified enzyme\*. J. Biol. Chem. 272 (23), 14727–14732.
- Takenaka, S., Okugawa, S., Kadowaki, M., Murakami, S., Aoki, K., 2003. The metabolic pathway of 4-aminophenol in *Burkholderia* sp. strain AK-5 differs from that of aniline and aniline with C-4 substituents. Appl. Environ. Microbiol. 69 (9), 5410–5413.
- Tamura, K., Stecher, G., Kumar, S., 2021. MEGA11: molecular evolutionary genetics analysis version 11. Mol. Biol. Evol. 38 (7), 3022–3027.
- Team, R.C. 2013. R: a language and environment for statistical computing.
- Wang, Y., Liu, K.F., Yang, Y., Davis, I., Liu, A., 2020. Observing 3-hydroxyanthranilate-3,4-dioxygenase in action through a crystalline lens. In: , 117, pp. 19720–19730.
- Wang, Y., Shin, I., Fu, Y., Colabroy, K.L., Liu, A., 2019. Crystal structures of L-DOPA dioxygenase from *Streptomyces sclerotialis*. Biochemistry 58 (52), 5339–5350.
- Wickham, H. and Wickham, M.H. 2007. The ggplot2 package. URL: <https://cran.r-project.org/web/packages/ggplot2/index.html>.
- Wilkinson-John, L., Boxall-Alistair, B.A., Kolpin-Dana, W., Leung-Kenneth, M.Y., Lai-Racliffe, W.S., Galbán-Malagón, C., Adell Aiko, D., Mondon, J., Metian, M., Marchant-Robert, A., Bouzas-Monroy, A., Cuni-Sanchez, A., Coors, A., Carriquiriborde, P., Rojo, M., Gordon, C., Cara, M., Moermond, M., Luarte, T., Petrosyan, V., Perikhanian, Y., Mahon-Clare, S., McGurk-Christopher, J., Hofmann, T., Kormoker, T., Iniguez, V., Guzman-Ortazo, J., Tavares-Jean, L., Gildasio-De-Figueiredo, F., Razzolini-Maria, T.P., Doughton, V., Gbaguidi, G., Traoré, O., Blais Jules, M., Kimpe Linda, E., Wong, M., Wong, D., Ntchantcho, R., Pizarro, J., Ying, G.G., Chen, C.E., Pérez, M., Martínez-Lara, J., Otamanga, J.-P., Poté, J., Ifo-Suspense, A., Wilson, P., Echeverría-Sáenz, S., Udikovic-Kolic, N., Milakovic, M., Fatta-Kassinos, D., Ioannou-Tfota, L., Belušová, V., Vymazal, J., Cárdenas-Bustamante, M., Kassa-Bayable, A., Garric, J., Chaumont, A., Gibba, P., Kunchulia, I., Seidensticker, S., Lyberatos, G., Halldórsson-Halldór, P., Melling, M., Shashidhar, T., Lamba, M., Nastiti, A., Supriatin, A., Pourang, N., Abedini, A., Abdullah, O., Gharbia-Salem, S., Pilla, F., Chefetz, B., Topaz, T., Yao-Koffi, M., Aurbakirova, B., Beisenova, R., Olaka, L., Mulu-Jemimah, K., Chatanga, P., Ntuli, V., Blama-Nathaniel, T., Sherif, S., Aris-Ahmad, Z., Looi-Ley, J., Niang, M., Traore-Seydou, T., Oldenkamp, R., Ogunbanwo, O., Ashfaq, M., Iqbal, M., Abdeen, Z., O'Dea, A., Morales-Saldaña-Jorge, M., Custodio, M., de la Cruz, H., Navarrete, I., Carvalho, F., Gogra, Alhaji, B., Koroma-Bashiru, M., Cerkenvenik-Flajs, V., Gombac, M., Thwala, M., Choi, K., Kang, H., Ladu-John, L.C., Rico, A., Amerasinghe, P., Sobek, A., Horlitz, G., Zenker-Armin, K., King Alex, C., Jiang, J.-J., Kariuki, R., Tumbo, M., Tezel, U., Onay-Turgut, T., Leiju-Julius, B., Vystavna, Y., Vergeles, Y., Heinzen, H., Pérez-Parada, A., Sims-Douglas, B., Figy, M., Good, D., Teta, C., 2022. Pharmaceutical pollution of the world's rivers. Proc. Natl. Acad. Sci. 119 (8), e2113947119.
- Wu, S., Zhang, L., Chen, J., 2012. Paracetamol in the environment and its degradation by microorganisms. Appl. Microbiol. Biotechnol. 96, 875–884.
- Wu, Y.W., Simmons, B.A., Singer, S.W., 2015. MaxBin 2.0: an automated binning algorithm to recover genomes from multiple metagenomic datasets. Bioinformatics 32 (4), 605–607.
- Yilmaz, P., Parfrey, L.W., Yarza, P., Gerken, J., Pruesse, E., Quast, C., Schweer, T., Peplies, J., Ludwig, W., Glöckner, F.O., 2014. The SILVA and "all-species living tree project (LTP)" taxonomic frameworks. Nucl. Acids Res. 42, D643–D648. Database issue.

- Yun, H., Liang, B., Qiu, J., Zhang, L., Zhao, Y., Jiang, J., Wang, A., 2017. Functional characterization of a novel amidase involved in biotransformation of triclocarban and its dehalogenated congeners in *Ochrobactrum* sp. TCC-2. *Environ. Sci. Technol.* 51 (1), 291–300.
- Zhang, J., Yin, J.G., Hang, B.J., Cai, S., He, J., Zhou, S.G., Li, S.P., 2012. Cloning of a novel arylamidase gene from *Paracoccus* sp. strain FLN-7 that hydrolyzes amide pesticides. *Appl. Environ. Microbiol.* 78 (14), 4848–4855.
- Zhang, L., Hang, P., Zhou, X., Dai, C., He, Z., Jiang, J., 2020. Mineralization of the herbicide swep by a two-strain consortium and characterization of a new amidase for hydrolyzing swep. *Microb. Cell Fact.* 19 (1), 4.
- Zhang, L., Hu, J., Zhu, R., Zhou, Q., Chen, J., 2013. Degradation of paracetamol by pure bacterial cultures and their microbial consortium. *Appl. Microbiol. Biotechnol.* 97 (8), 3687–3698.
- Zhang, L., Hu, Q., Hang, P., Zhou, X., Jiang, J., 2019. Characterization of an arylamidase from a newly isolated propanil-transforming strain of *Ochrobactrum* sp. PP-2. *Ecotoxicol. Environ. Saf.* 167, 122–129.
- Zou, D., Huang, Y., Liu, W., Yang, Z., Dong, D., Huang, S., He, X., Ao, D., Liu, N., Wang, S., Wang, Y., Tong, Y., Yuan, J., Huang, L., 2017. Complete sequences of two novel bla (NDM-1)-harbouring plasmids from two *Acinetobacter towneri* isolates in China associated with the acquisition of Tn125. *Sci. Rep.* 7 (1), 9405.
- Żur, J., Piński, A., Marchlewicz, A., Hupert-Kocurek, K., Wojcieszynska, D., Guzik, U., 2018a. Organic micropollutants paracetamol and ibuprofen—toxicity, biodegradation, and genetic background of their utilization by bacteria. *Environ. Sci. Pollut. Res.* 25 (22), 21498–21524.
- Żur, J., Wojcieszynska, D., Hupert-Kocurek, K., Marchlewicz, A., Guzik, U., 2018b. Paracetamol – toxicity and microbial utilization. *Pseudomonas moorei* KB4 as a case study for exploring degradation pathway. *Chemosphere* 206, 192–202.